Spatial and temporal variations in denudation of the Wasatch Mountains, Utah, USA

Greg M. Stock[1]*, Kurt L. Frankel[2]*, Todd A. Ehlers[3], Mirjam Schaller[3], Stephanie M. Briggs[4], and Robert C. Finkel[5]
[1]DIVISION OF RESOURCES MANAGEMENT AND SCIENCE, YOSEMITE NATIONAL PARK, EL PORTAL, CALIFORNIA 95318, USA
[2]SCHOOL OF EARTH AND ATMOSPHERIC SCIENCES, GEORGIA INSTITUTE OF TECHNOLOGY, ATLANTA, GEORGIA 30332-0340, USA
[3]DEPARTMENT OF GEOLOGICAL SCIENCES, UNIVERSITY OF MICHIGAN, ANN ARBOR, MICHIGAN 48109-1005, USA
[4]WILLIAM LETTIS AND ASSOCIATES, INC., AUGUSTA, GEORGIA 30901-0851, USA
[5]DEPARTMENT OF EARTH AND PLANETARY SCIENCES, UNIVERSITY OF CALIFORNIA, BERKELEY, CALIFORNIA 94720-4767, USA, *AND* CENTRE EUROPÉEN DE RECHERCHE ET D'ENSELIGNEMENT DES GÉOSCIENCES DE L'ENVIRONNEMENT (CEREGE), 13545 AIX EN PROVENCE, FRANCE

ABSTRACT

We evaluate spatial and temporal variations in denudation of the north-central Wasatch Mountains, Utah, by determining catchment-wide denudation rates with ^{10}Be concentrations in alluvial sediment and comparing these rates with previously published data on rock uplift and exhumation of the range. Catchments draining the range front show relatively little variation in denudation rate (0.07–0.17 mm/yr), while steeper (mean hillslope gradient >30°) catchments in the core of the range show larger variation (0.17–0.79 mm/yr). We attribute the larger spatial variation in catchment-wide denudation in the core of the range to landsliding of hillslopes at threshold gradients; faster denudation in this region may signify landscape adjustment to late Pleistocene glaciations. The mean denudation rate for all catchments (0.2 mm/yr) is generally consistent with longer-term exhumation rates derived from thermochronometers and with shorter-term vertical fault displacement rates, suggesting that denudation of the north-central Wasatch has been roughly steady, or decreasing slightly, over the past 5 m.y. Although ^{10}Be-based catchment-wide denudation rates are sensitive to localized geomorphic processes and events, overall, they appear to reflect the larger tectonic forces that have driven denudation of the Wasatch Mountains over longer time scales.

LITHOSPHERE; v. 1; no. 1; p. 34–40. doi: 10.1130/L15.1

INTRODUCTION

Quantification of spatial and temporal variations in denudation of tectonically active areas can provide key insights into mountain belt evolution. For example, spatial variability in mountain denudation rates can help identify tectonically active structures and determine surface uplift rates. Temporal variability can reveal the timing of tectonic events and can clarify the relative roles that tectonics and climate play in driving rock uplift and denudation of orogens. Long temporal records of denudation also provide a means of assessing the steadiness of mountain erosion and topography through time.

Spatial variations in denudation rate can be quantified simply by collecting samples distributed across a broad region, but temporal variations are more challenging, requiring measurements over different time scales. Rates of long-term rock exhumation are often inferred from zircon fission-track (ZFT), apatite fission-track (AFT), and apatite (U-Th)/He (AHe) thermochronometers, which average denudation over relatively long time scales (10^5–10^8 yr) (e.g., Ehlers and Farley, 2003; Reiners and Brandon, 2006). Over shorter time scales (10^2–10^5 yr), denudation rates can be determined using cosmogenic nuclides such as ^{10}Be (e.g., Gosse and Phillips, 2001). Beryllium-10 concentrations in alluvial sediment are particularly useful indicators of landscape-scale denudation because alluvial sediment is generally thought to integrate catchment-wide denudation signals (e.g., Bierman and Steig, 1996; Granger et al., 1996; Schaller et al., 2001; von Blanckenburg, 2005; Schaller and Ehlers, 2006). Spatial variations in catchment-wide denudation can be related to the proximity of tectonically active structures (Wobus et al., 2005). Furthermore, catchment-wide denudation rates derived from cosmogenic nuclides can be compared to long-term rock exhumation rates derived from thermochronometers to evaluate temporal variations in denudation (e.g., Kirchner et al., 2001; Matmon et al., 2003; Vance et al., 2003; Wittmann et al., 2007; Cyr and Granger, 2008), providing insights into mountain belt evolution. However, because these methods average denudation over different time periods, they have differing sensitivities to geomorphic processes; the degree to which these factors affect direct comparisons between geochronometers has not been fully explored.

We investigated spatial and temporal variations in denudation of the north-central Wasatch Mountains, an area with a high density and quality of existing geochronologic data. Our objectives were twofold: (1) to evaluate spatial variations in catchment-wide denudation rates derived from cosmogenic ^{10}Be concentrations in alluvial sediment, specifically testing whether erosion rates correlate with proximity to or distance along the range front fault, and (2) to evaluate temporal variations in denudation of the Wasatch Mountains by comparing our ^{10}Be-based catchment-wide denudation rates with previously published long-term exhumation rates derived from thermochronometers and with shorter-term vertical fault displacement rates.

GEOLOGIC SETTING OF THE NORTH-CENTRAL WASATCH MOUNTAINS

The Wasatch Mountains, reaching >3.4 km in altitude, have been uplifted in the footwall of the west-dipping Wasatch fault zone (Fig. 1), one of the most extensively studied segmented normal faults in the world.

*E-mails: greg_stock@nps.gov, kfrankel@gatech.edu.

The Wasatch fault zone is an active normal fault system composed of at least six segments; the Salt Lake City and Weber segments bound our study area on the west (Fig. 1). Deformation initiated on the Wasatch fault in the past 12–17 m.y. and continues today (Friedrich et al., 2003; Machette et al., 1992). The total magnitude of exhumation in the central Wasatch adjacent to the Salt Lake City segment is estimated to be ~11 km (Ehlers et al., 2003; Parry and Bruhn, 1987). Rock uplift along the Wasatch fault occurs as tilt about a footwall hinge located ~20–25 km east of the fault (Ehlers et al., 2003). Rocks in the footwall of the Salt Lake City segment are composed primarily of granitic rocks from the Oligocene-age Little Cottonwood Stock, with lesser amounts of quartzites, shales, and siltstones of the middle Proterozoic–age Big Cottonwood Formation (Bryant, 1990; Ehlers and Chan, 1999). Rocks in the footwall of the Weber segment are mainly gneisses and granitic rocks of the middle Precambrian Farmington Canyon Complex (Davis, 1983). Quaternary fluvial, colluvial, glacial, and lacustrine deposits are present in both areas; along the Weber segment, glacial material is found only east of the range crest (Davis, 1983).

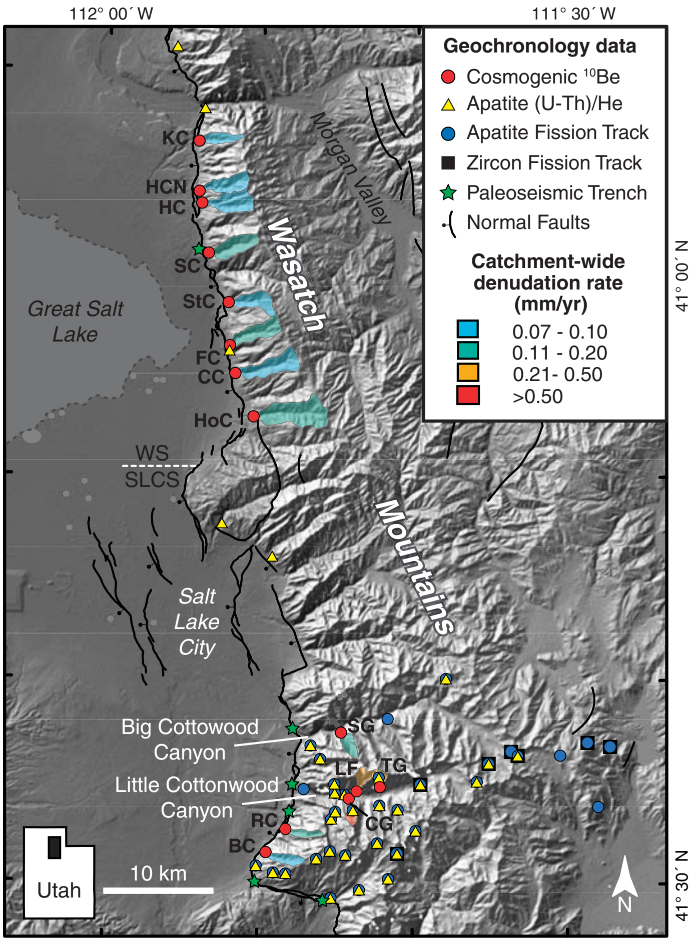

Figure 1. Salt Lake City and Weber segments of Wasatch fault zone and adjacent Wasatch Mountains showing ^{10}Be sample locations (this study), thermochronometer samples (Armstrong et al., 2003, 2004), and paleoseismic study sites (Machette et al., 1992; McCalpin and Nishenko, 1996; Nelson and Personius, 1993). Sampled catchments are colored according to their denudation rate. Tick marks on faults are located on the hanging wall. Horizontal, white, dashed line delineates boundary between Weber and Salt Lake City segments of Wasatch fault zone. Faults are from U.S. Geological Survey Quaternary Fault and Fold Database (http://earthquake.usgs.gov/regional/qfaults/). WS—Weber segment of the Wasatch fault zone, SLCS—Salt Lake City segment of the Wasatch fault zone; KC—Kays Creek North, HCN—Holmes Creek North, HC—Holmes Creek, SC—Shepards Creek, StC—Steed Creek, FC—Ford Canyon, CC—Centerville Canyon, HoC—Holbrook Creek, SG—Stairs Gulch, LF—Lisa Falls, TG—Tanner Gulch, CG—Coalpit Gulch, RC—Rocky Mouth Creek, BC—Bear Creek.

Previous studies have used ZFT, AFT, and AHe thermochronometry to study the exhumation history of the Wasatch fault footwall (Fig. 1) (Naeser et al., 1983; Kowallis et al., 1990; Ehlers et al., 2003; Armstrong et al., 2003, 2004). Coupled two-dimensional thermokinematic and age prediction models suggest exhumation rates of <0.2–0.4 mm/yr over the past 5 m.y. for most of the Wasatch front, including the Weber and northern Salt Lake City segments (Ehlers et al., 2003; Armstrong et al., 2004). These rates agree with a rate of ~0.4 mm/yr for the Weber segment determined from AFT ages (Naeser et al., 1983). The exception is the central Wasatch along the southern Salt Lake City segment, where exhumation rates are apparently more rapid, at 0.6–0.8 mm/yr (Ehlers et al., 2003; Armstrong et al., 2004). This region corresponds to the highest peak elevations and greatest topographic relief in our study area. Assuming that exhumation rates in this setting are driven in the long term by rock uplift, rates of rock uplift along the Wasatch fault appear to be similar across fault segments at <0.2–0.4 mm/yr, except for the more rapidly uplifting southern Salt Lake City segment. Spatial exhumation patterns suggest strong tectonic forcing; maximum exhumation rates occur at the range front fault and decrease linearly to 0 mm/yr at the footwall hinge (Ehlers et al., 2003).

Fault trench studies along the Salt Lake City segment suggest an average net tectonic vertical displacement rate (the relative vertical distance between the hanging wall and footwall following an earthquake) of 1.0–1.7 mm/yr over the past ~6 k.y. (Friedrich et al., 2003). Paleoseismic studies and scarp profile analyses of the Weber segment yield a vertical displacement rate of 1.2 +3.1/–0.6 mm/yr over the past ~18 k.y., where rates are highest in the center and decrease toward the northern and southern tips of the Weber segment (Nelson and Personius, 1993; Lund, 2005, and references therein). However, older offset alluvial fans suggest that the average vertical displacement rate on the Salt Lake City segment since ca. 250 ka is much slower, at 0.1–0.3 mm/yr (Machette, 1981; Machette et al., 1992), which is consistent with other estimates of late Pleistocene vertical displacement rates on Wasatch fault segments (Niemi et al., 2004) and more similar to longer-term exhumation rates.

BERYLLIUM-10–DERIVED CATCHMENT DENUDATION RATES

We determined catchment-wide denudation rates in the north-central Wasatch by measuring ^{10}Be concentrations in alluvial sediment exiting catchments. To reduce the number of variables affecting catchment denudation rates, and thus make meaningful comparisons with longer-term rock exhumation rates and shorter-term fault displacement rates, we developed strict criteria to guide our sampling. We restricted our sampling to catchments that: (1) were of similar size; (2) had similar underlying lithologies; (3) were within areas previously sampled for thermochronometry; (4) were positioned at varying distances along and perpendicular to the Wasatch fault; and (5) were not extensively glaciated (<10% of the total catchment area) during the latest Pleistocene or Holocene (Laabs et al., 2006; Madsen and Currey, 1979; Davis, 1983). This last criterion is important because cosmogenic nuclide exposure histories from glaciated catchments likely do not satisfy steady-state denudation assumptions due to ice shielding during erosion, prolonged sediment storage, and/or fluvial reworking of glacially derived sediment (e.g., Wittmann et al., 2007).

We sampled 14 catchments that fulfilled these criteria. The catchments drain the range front along both the Weber and Salt Lake City fault

TABLE 1. SAMPLE LOCATIONS AND TOPOGRAPHIC METRICS FOR WASATCH MOUNTAINS CATCHMENTS

Catchment name	Catchment abbreviation	Latitude (°N)	Longitude (°W)	Fault segment	Distance from fault (km)	Distance along fault (km)*	Area (km^2)	Elevation range (km)†	Relief (km)§	Mean hillslope (°)#
Kays Creek North	KC	41.12	111.84	Weber	0.53	3.7	3.23	1.61–2.72 (2.17)	1.11	26
Holmes Creek North	HCN	41.07	111.84	Weber	0.65	7.8	5.82	1.55–2.95 (2.29)	1.40	31
Holmes Creek	HC	41.06	111.84	Weber	0.37	8.9	7.10	1.57–2.89 (2.31)	1.32	29
Shepards Creek	SC	41.01	111.84	Weber	0.59	13.4	6.12	1.48–2.88 (2.15)	1.40	29
Steed Creek	StC	40.97	111.84	Weber	0.46	17.9	7.00	1.49–2.82 (2.24)	1.33	28
Ford Canyon	FC	40.94	111.87	Weber	0.42	21.9	6.85	1.49–2.82 (2.24)	1.33	25
Centerville Creek	CC	40.91	111.86	Weber	0.36	24.3	8.50	1.51–2.67 (2.13)	1.16	26
Holbrook Creek	HoC	40.88	111.84	Weber	1.05	28.2	13.51	1.55–2.82 (2.23)	1.27	25
Stairs Gulch	SG	40.62	111.74	Salt Lake	4.06	28.2	2.42	1.81–3.21 (2.50)	1.40	42
Lisa Falls	LF	40.57	111.73	Salt Lake	5.45	34.0	2.17	2.04–3.46 (2.87)	1.42	40
Tanner Gulch	TG	40.58	111.70	Salt Lake	7.46	34.0	1.84	2.19–3.43 (2.86)	1.24	42
Coalpit Gulch	CG	40.57	111.74	Salt Lake	4.62	34.0	2.05	1.89–3.37 (2.74)	1.48	41
Rocky Mouth Creek	RC	40.54	111.80	Salt Lake	0.30	37.4	2.24	1.61–3.14 (2.41)	1.53	31
Bear Creek	BC	40.52	111.82	Salt Lake	0.34	40.4	3.14	1.57–2.92 (2.36)	1.35	32

*Distance along trace of Weber and Salt Lake City fault segments, respectively, from north to south.
†Minimum (sample location) and maximum catchment elevations; mean catchment elevation is shown in parentheses.
§Catchment relief calculated as the difference between the minimum and maximum catchment elevations.
#Mean catchment slope calculated as the maximum change in elevation in the east-west or north-south direction in a three-cell by three-cell (30 × 30 m) moving window by fitting a plane to elevation values; slope value in degrees is reported for the central cell in the three-cell by three-cell neighborhood.

segments, and also tributaries to Big Cottonwood and Little Cottonwood Canyons within the core of the central part of the range, adjacent to the Salt Lake City segment (Fig. 1). Thirteen of the sampled catchments are incised predominantly or entirely into granitic rocks of the Little Cottonwood Stock or Farmington Canyon Complex, from which most thermochronometry samples were collected (Armstrong et al., 2003, 2004); the exception, Stairs Gulch, is cut into quartzites of the Big Cottonwood Formation. Catchment relief (the difference between the minimum and maximum elevation within a catchment) ranges from 1.07 to 1.50 km (Table 1). Mean hillslope gradients range from 26° to 43°, and the steeper catchments occur in the core of the range (Table 1; Fig. 1). Based on field observations of the amount of bedrock exposed in channels, the sampled catchments appear to be either primarily detachment (weathering)–limited or intermediate between detachment-limited and transport-limited (cf. Howard et al., 1994). Annual precipitation in the study area ranges from ~500 mm/yr near the range front to ~1400 mm/yr near the range crest (Western Region Regional Climate Center, www.wrcc.dri.edu).

We collected alluvial sediment from the active channel just upstream of each catchment outlet. For the catchments draining the range front, we sampled upstream of the highest Lake Bonneville shoreline to preclude reworking of beach sediments. We processed the 2–4 mm grain size fraction for the Salt Lake City segment catchments and the 0.25–0.5 mm grain size fraction for the Weber segment catchments. Different hillslope denudation processes acting over varying time scales can contribute different sediment grain sizes to fluvial systems. Recognizing that grain size can potentially affect ^{10}Be concentration (e.g., Belmont et al., 2007; Matmon et al., 2003; Brown et al., 1998), we processed both grain size fractions from one catchment (Rocky Mouth Creek) as a basis for comparison. As shown in Table 2, ^{10}Be concentrations for the two size fractions from this catchment are identical within analytical uncertainty, increasing our confidence that catchment-wide denudation rates are comparable between the Salt Lake City and Weber segment catchments.

We determined ^{10}Be production rates for each sampled catchment using a 10-m-resolution digital elevation model (DEM) of the study area

TABLE 2. BERYLLIUM-10 ANALYTICAL DATA AND DENUDATION RATES FOR WASATCH MOUNTAINS CATCHMENTS

Catchment name	Catchment abbreviation	Mass quartz (g)	Mass Be carrier (g)*	^{10}Be/^{9}Be ($\times10^{-13}$)†	Snow shielding factor	P_{10} (atoms g^{-1} yr^{-1})§	^{10}Be ($\times10^{4}$ atoms g^{-1})	Denudation rate (mm/yr)#	Denudation time scale (yr)
Kays Creek North	KC	56.10	0.3059	6.66 – 0.16	0.98	26.2	23.98 – 0.62	0.07 – 0.01	9000
Holmes Creek North	HCN	52.99	0.3057	7.17 – 0.17	0.97	28.5	27.33 – 0.71	0.07 – 0.01	9500
Holmes Creek	HC	60.01	0.3059	5.84 – 0.21	0.97	28.6	19.61 – 0.74	0.10 – 0.01	6800
Shepards Creek	SC	50.01	0.3104	3.19 – 0.09	0.98	26.0	12.84 – 0.39	0.14 – 0.01	4800
Steed Creek	StC	70.59	0.3071	7.89 – 0.20	0.98	27.3	22.70 – 0.62	0.08 – 0.01	8200
Ford Canyon	FC	70.07	0.3058	5.47 – 0.14	0.98	27.4	15.73 – 0.44	0.12 – 0.01	5700
Centerville Creek	CC	70.02	0.3078	7.69 – 0.23	0.98	25.4	22.35 – 0.72	0.08 – 0.01	8700
Holbrook Creek	HoC	65.02	0.3060	5.58 – 0.11	0.98	27.1	17.30 – 0.39	0.11 – 0.01	6300
Stairs Gulch	SG	57.26	0.2658	3.15 – 0.26	0.95	27.4	10.93 – 0.91	0.17 – 0.01	4000
Lisa Falls	LF	153.62	0.3064	3.92 – 0.54	0.89	34.9	5.07 – 0.71	0.46 – 0.06	1500
Tanner Gulch	TG	112.34	0.2643	3.22 – 0.22	0.88	34.0	4.91 – 0.34	0.46 – 0.03	1500
Coalpit Gulch	CG	57.79	0.2694	1.08 – 0.08	0.89	34.6	2.93 – 0.22	0.79 – 0.07	900
Rocky Mouth Creek	RC	78.52	0.3011	5.46 – 0.13	0.97	30.5	12.02 – 0.31	0.17 – 0.01	3900
Rocky Mouth Creek	RC	54.68	0.3024	3.73 – 0.09	0.97	30.5	11.82 – 0.31	0.17 – 0.01	3900
Bear Creek	BC	140.67	0.3059	12.56 – 0.54	0.99	27.3	18.22 – 0.79	0.10 – 0.01	6700

*Be carrier concentration of 1000 µg/mL.
†^{10}Be/^{9}Be ratios measured against NIST (KC, HCN, HC, SC, StC, FC, CC, HoC, and RC) and revised ICN (SG, LF, TG, CG, and BC) standards, normalized to the NIST standard (Nishiizumi et al., 2007). Uncertainty is 1σ analytical uncertainty.
§Catchment-wide ^{10}Be production rate, incorporating (1) nucleonic production (5.1 ± 0.3 atom g^{-1} yr^{-1}; Stone, 2000) scaled for latitude, altitude, topographic shielding, and snow shielding and decreasing exponentially with depth below ground surface, and (2) muogenic production (0.093 atoms g^{-1} yr^{-1} for fast muons [Heisinger et al., 2002a]; 0.106 atoms g^{-1} yr^{-1} for negative muon capture [Heisinger et al., 2002b]) scaled for altitude only and decreasing exponentially with depth below ground surface.
#Denudation rates calculated assuming a ^{10}Be half-life of 1.36 ± 0.07 m.y. (Nishiizumi et al., 2007).

and calculating local ^{10}Be production rates, scaled for latitude, altitude, and topographic shielding, for each DEM pixel. Since the north-central Wasatch receives abundant winter snow that is highly dependent on elevation, we calculated snow shielding factors (e.g., Gosse and Phillips, 2001) for each DEM pixel using local monthly precipitation-elevation and temperature-elevation regressions (Laabs et al., 2006). Snow shielding proved to be significant for catchments in the core of the range, with snow shielding factors as low as 0.88 (Table 2). Although the climate data used to calculate snow shielding only span ≤50 yr, we do not expect large variations in snowfall for the Holocene time scales over which our denudation rates are integrated. Multiplication of production rates by snow shielding factors yielded the final catchment-wide ^{10}Be production rates (Table 2). Our calculations of catchment-wide denudation rates assume steady, uniform erosion from all DEM pixels for which ^{10}Be production rates were calculated. Although we did not specifically test this assumption, nonglaciated catchments with similar metrics elsewhere in the Basin and Range Province have been shown to be eroding uniformly (Stock et al., 2006).

RESULTS AND DISCUSSION

Spatial Variations in Denudation Rate

Beryllium-10–based denudation rates for the sampled catchments vary by roughly an order of magnitude, ranging from 0.07 to 0.79 mm/yr (Table 2). Spatial variation in denudation along the range front, spanning both the Salt Lake City and Weber fault segments, is relatively small; rates range from 0.07 to 0.17 mm/yr (Fig. 2). However, denudation rates from catchments within the core of the range along the Salt Lake City segment are much more variable, ranging from 0.17 to 0.79 mm/yr (Fig. 2).

Given that rock uplift rates and thermochronometer-derived exhumation rates are at maximum values adjacent to the range front fault (Armstrong et al., 2003; Ehlers et al., 2003), catchments draining the range front might be expected to display faster ^{10}Be-based catchment-wide denudation rates than those in the core of the range. On the contrary, we find that catchments along the range front display the slowest denudation rates (Fig. 2); catchments draining the range front ($n = 10$) yield a mean denudation rate of 0.10 mm/yr, while catchments in the core of the range ($n = 4$) yield a mean denudation rate of 0.47 mm/yr (Tables 1 and 2; Fig. 2). There is only weak correlation of denudation rates with along-strike variations in fault slip rate, despite previous work suggesting that tectonic activity controls landscape development in the Wasatch footwall (Frankel and Pazzaglia, 2005). As denudation rates are not strongly correlated with proximity to, or distance along, the range front fault, localized tectonic forcing does not appear to exert strong control on the spatial distribution of catchment-wide denudation rates in this setting, at least on the Holocene time scales over which these measurements are made. Although tectonic forcing probably drives landscape-scale denudation of the Wasatch Mountains, localized geomorphic processes and events, acting in response to this forcing, appear to exert stronger first-order control on the spatial distribution of catchment-wide denudation rates over shorter time scales.

The geomorphic processes that accomplish catchment denudation are often associated with topographic metrics such as catchment area, relief, elevation, and hillslope gradient (e.g., Ahnert, 1970; Montgomery and Brandon, 2002; Roering et al., 2007). In our study area, catchment-wide denudation rates are poorly correlated with catchment relief (Fig. 3C). Denudation rates are moderately correlated with mean catchment elevation (Fig. 3B), suggesting that elevation-dependent processes (e.g., frost cracking; Hales and Roering, 2007) may be important in driving denudation in these primarily detachment-limited catchments. Catchment-wide denudation rates are also moderately correlated with mean hillslope gradient, though the correlation is valid only at lower hillslope gradients and denudation rates; for hillslope gradients >30°, denudation rates show considerable scatter (Fig. 3D). The nonlinear relationship between mean hillslope gradient and denudation rate has been observed in other data sets (e.g., Roering et al., 2001; Montgomery and Brandon, 2002; Binnie et al., 2007) and has been attributed to hillslopes reaching a threshold condition, above which mass-wasting processes dominate hillslope processes (Burbank et al., 1996). We conclude that the relatively large spatial variation in catchment-wide denudation rates in the core of the range is likely due to discrete landslide events occurring on hillslopes at threshold gradients. Landslide events are sediment point sources, so they violate assumptions of steady, uniform erosion implicit in the catchment-wide denudation rate calculations from ^{10}Be concentrations; thus, landslides can skew short-term catchment-wide denudation rates (Niemi et al., 2005; Belmont et al., 2007). Denudation rates may be faster in catchments with smaller contributing areas (Fig. 3A) because the effects of landslides on ^{10}Be concentrations in alluvium are proportionally greater in smaller catchments. Although the extent of landslide activity in our study area has not been quantified, we did observe isolated fresh talus deposits in those catchments draining to Little Cottonwood Canyon (Fig. 1).

Cosmogenic nuclide concentrations are generally not sensitive to glacial-interglacial fluctuations except at high (>0.5 mm/yr) denudation rates (Schaller and Ehlers, 2006), but they can record landscape adjustments to glacial erosion. Much of the core of the north-central Wasatch, including Little Cottonwood Canyon, contained large trunk glaciers during the Last Glacial Maximum (Madsen and Currey, 1979; Laabs et al., 2006). Glacial erosion in the major canyons likely deepened these canyons, inciting accelerated denudation in tributary catchments. Prominent (>10 m) knickpoints are not apparent in the DEM-derived longitudinal channel profiles of tributary catchments to Little Cottonwood Canyon, but field observations indicate numerous smaller (<10 m) knickpoints, which may be significant at the scale of these catchments. Thus, the discrepancy between faster exhumation rates at the range front over long time scales, as recorded by

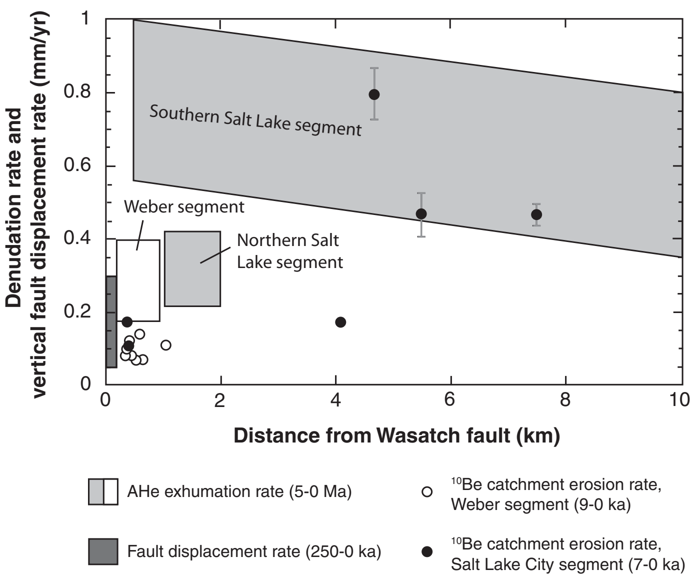

Figure 2. Spatial variation in catchment denudation, rock exhumation, and vertical fault displacement rates as a function of distance from the range front Wasatch fault. AHe-based exhumation rates, shown by white (Weber segment) and light gray (Salt Lake City segment) boxes, are from Armstrong et al. (2003, 2004) and Ehlers et al. (2003). Vertical fault displacement rates (dark gray box) are from Machette et al. (1992) and Friedrich et al. (2003).

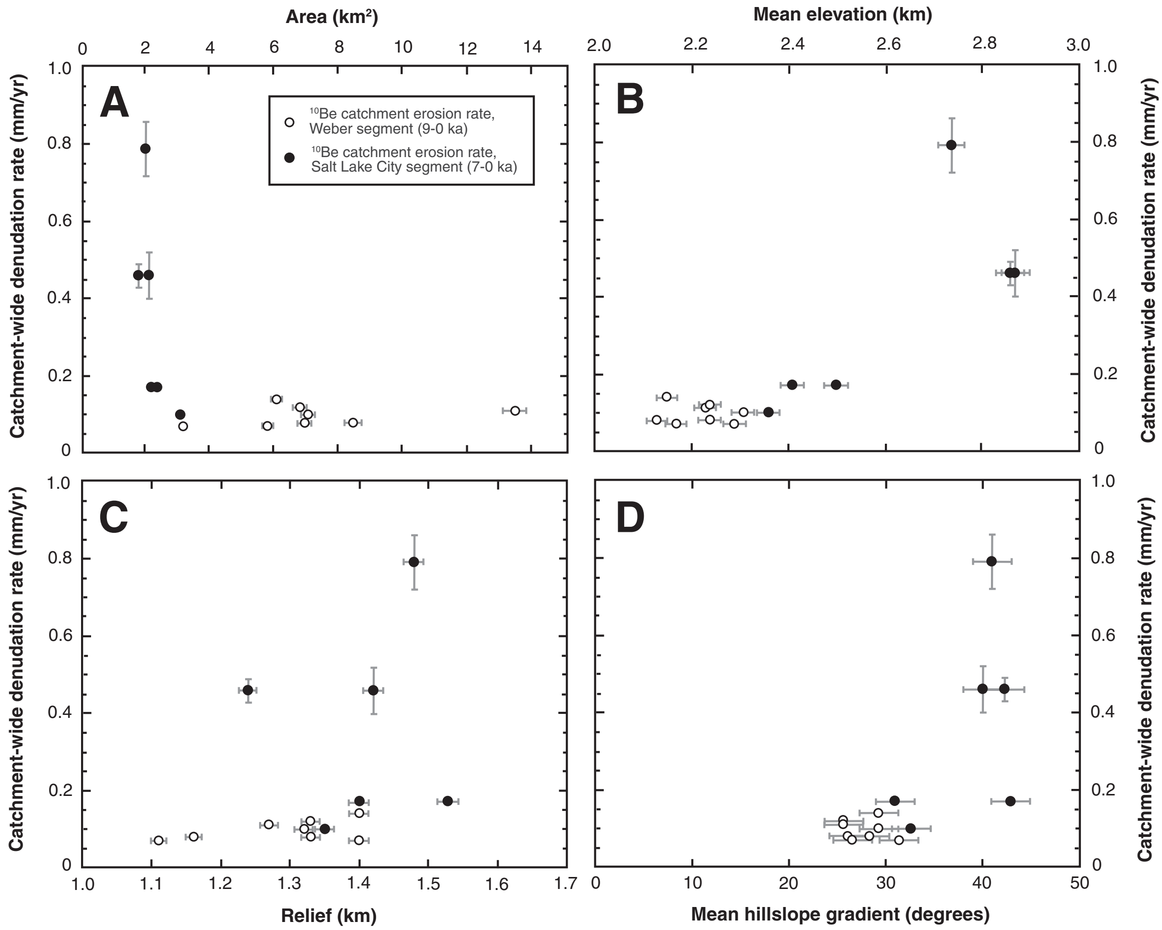

Figure 3. Catchment-wide denudation rates derived from cosmogenic ^{10}Be as a function of (A) catchment area, (B) mean elevation, (C) catchment relief, and (D) mean hillslope angle. Horizontal error bars represent 2σ uncertainty in digital elevation model (DEM) analyses (Frankel and Pazzaglia, 2005); vertical error bars represent propagated 1σ analytical uncertainty in ^{10}Be-based denudation rates; where not shown, error bars are smaller than marker symbols.

thermochronometers, and faster denudation rates in the core of the range over shorter time scales, as recorded by cosmogenic ^{10}Be, may relate to the lingering effects of late Pleistocene glaciations in this part of our study area. We posit that landsliding in those sampled catchments draining to Little Cottonwood Canyon (Lisa Falls, Tanner Gulch, and Coalpit Gulch) may be accelerated due to late Pleistocene glacial valley deepening.

Temporal Variations in Denudation Rate

In primarily nonglacial catchments like those sampled, channel incision sets the pace at which hillslopes are eroded, which in turn drives overall denudation of landscapes (i.e., rock exhumation). In a landscape experiencing steady denudation over long time periods (e.g., Willett and Brandon, 2002), shorter-term ^{10}Be-based catchment-wide denudation rates should be similar to longer-term thermochronometer-derived exhumation rates. If denudation is driven primarily by rock uplift and/or base-level fall, and rock uplift and denudation are in equilibrium, catchment-wide denudation rates should also be similar to vertical fault displacement rates.

This situation appears to be borne out by our data from the north-central Wasatch. The mean denudation rate for all sampled catchments is 0.2 ± 0.2 mm/yr, time-averaged over ~5 k.y. (Table 2). This rate is consistent with exhumation rates of <0.2–0.4 mm/yr over the past 5 m.y. for most of the Wasatch front, including the Weber and northern Salt Lake City segments (Ehlers et al., 2003; Armstrong et al., 2004; Naeser et al., 1983). It is also consistent with exhumation estimates derived from fluid inclusions (<0.5 mm/yr since ca. 5 Ma; Parry and Bruhn, 1987). The mean catchment-wide denudation rate is fully consistent with late Pleistocene vertical displacement rates on the Salt Lake segment (0.1–0.3 mm/yr) and other segments (0.2–0.4 mm/yr) of the Wasatch fault (Machette et al., 1992; Mattson and Bruhn, 2001) (Fig. 2). Only at the shortest time scales is there a substantial difference between catchment-wide denudation rates and vertical displacement rates; the mean catchment erosion rate of 0.2 mm/yr is considerably slower than Holocene vertical displacement rates on the Salt Lake (1.7 mm/yr over the past ~6 k.y.) and Weber fault segments (~1.2 mm/yr since 7.9 ka; Friedrich et al., 2003; McCalpin and Nishenko, 1996). However, these displacement rates are considered to be anomalous because of clustered seismic strain release during this relatively short time interval (Chang and Smith, 2002; Friedrich et al., 2003; Niemi et al., 2004). The fact that ^{10}Be-based catchment-wide denudation rates are roughly an order of magnitude slower than Holocene vertical fault displacement rates, and are instead similar to longer-term (~250 k.y.) displacement rates, suggests that the north-central Wasatch landscape is apparently not sensitive to short-term (10^3 yr) perturbations. Instead, the Wasatch Mountains are influenced by longer-term tectonic signals (cf. Whipple, 2001) and landscape response times that are greater than the recurrence interval of individual seismic events or earthquake clusters.

The similarity of denudation rates over long time scales is striking considering that there are fundamental differences in the ways in which the various geochronometers record denudation. For example, thermochronometer-derived denudation rates include uncertainties in the kinetics of He diffusion in apatite (e.g., Farley, 2000) and potentially oversimplified assumptions regarding the thermal field through which bedrock samples cool (e.g., Ehlers, 2005; Braun, 2005). The ^{10}Be-based denudation rates include uncertainties in ^{10}Be production rates (e.g., Gosse and Phillips, 2001) and potentially oversimplified assumptions regarding steady, uniform erosion of catchments. Averaged over long time scales, thermochronometer-based denudation rates are largely insensitive to discrete tectonic (e.g., individual earthquake), climatic (e.g., glacial-interglacial cycles), and geomorphic (e.g., individual landslide) events. In contrast, ^{10}Be-based denudation rates may be quite sensitive to these events.

In landscapes that denude predominantly during stochastic events such as landslides, individual ^{10}Be-based catchment-wide denudation rate measurements are more likely to be skewed away from the longer-term denudation rate as measured by thermochronometers. Thus, even in cases of erosional steady state, ^{10}Be-based denudation rates will probably show greater scatter about the mean long-term rate. In this case, the mean catchment-wide denudation rate for our study area is generally consistent with results from other geochronometers. Direct comparisons of ^{10}Be-based catchment-wide denudation rates with longer-term thermochronometer-based rates at the range front suggest that denudation of the Wasatch Mountains has been roughly steady, perhaps slightly decreasing along the southern Salt Lake City segment, over the past 5 m.y. Ultimately, when comparing denudation rates derived from different geochronometers, it is important to consider the underlying assumptions of the various methods, the sensitivity of those methods to individual geomorphic events, the amount of time over which denudation rates are averaged, and the number of samples necessary to adequately capture signals of mountain denudation.

CONCLUSIONS

Cosmogenic ^{10}Be concentrations in alluvial sediment from the north-central Wasatch Mountains indicate catchment-wide denudation rates of 0.07–0.79 mm/yr. Denudation rates along the range front are relatively uniform, between 0.07 and 0.17 mm/yr (mean 0.10 mm/yr), while steeper catchments within the core of the range show greater variation, between 0.17 and 0.79 mm/yr, and overall faster rates (mean 0.47 mm/yr). Unlike thermochronometer-derived exhumation rates, ^{10}Be-based catchment-wide denudation rates do not display a spatial distribution strongly influenced by localized tectonic forcing (i.e., faster denudation rates adjacent to the range front fault). Faster and more variable denudation rates in the core of the range likely relate to higher hillslope gradients that are at (or near) threshold values for landsliding. We suggest that denudation rates are higher in the core of the range because landscapes there are still adjusting to changes incurred by late Pleistocene glaciations.

The mean denudation rate for all sampled catchments (0.2 mm/yr) is generally consistent with both longer-term exhumation rates and shorter-term vertical fault displacement rates, suggesting that denudation of the north-central Wasatch has been roughly steady, or decreasing slightly, over the past 5 m.y. Because thermochronometers average denudation over long time scales, they generally record rock exhumation without regard to specific geomorphic processes, and therefore they provide relatively stable estimates of long-term erosion. In contrast, cosmogenic nuclide concentrations in alluvial sediment average denudation over shorter time scales and can be highly sensitive to localized geomorphic processes and events. We conclude that although ^{10}Be-based catchment-wide denudation rates are sensitive to these events, taken as a whole, they appear to reflect the large-scale tectonic forces that have driven denudation of the north-central Wasatch Mountains over the past 5 m.y.

ACKNOWLEDGMENTS

We thank Dave Whipp and Matt Densmore for field assistance, Erin Bachynski and Alicia Nobles for analytical assistance, and Frank Pazzaglia and James Dolan for discussions and support. Greg Balco wrote the Matlab code used to calculate catchment-averaged ^{10}Be production rates. Beryllium-10 measurements were made at PRIME Lab and Lawrence Livermore National Laboratory (LLNL). We thank Arjun Heimsath, Darryl Granger, and editor Jon Pelletier for helpful comments that improved the paper. This work was supported by National Science Foundation (NSF) grant EAR-0544954 (Ehlers and Stock), an LLNL-UEPP Fellowship (Frankel), and grants from the Georgia Tech Research Foundation and the Colorado Scientific Society (Frankel).

REFERENCES CITED

Ahnert, F., 1970, Functional relationship between denudation, relief, and uplift in large mid-latitude drainage basins: American Journal of Science, v. 268, p. 243–263.

Armstrong, P.A., Ehlers, T.A., Chapman, D.S., Farley, K.A., and Kamp, P.J.J., 2003, Exhumation of the central Wasatch Mountains, Utah: 1. Patterns and timing deduced from low-temperature thermochronology data: Journal of Geophysical Research, v. 108, doi: 10.1029/2001JB001708.

Armstrong, P.A., Taylor, A.R., and Ehlers, T.A., 2004, Is the Wasatch fault footwall (Utah, United States) segmented over million-year time scales?: Geology, v. 32, p. 385–388, doi: 10.1130/G20421.1.

Belmont, P., Pazzaglia, F.J., and Gosse, J.C., 2007, Cosmogenic ^{10}Be as a tracer for hillslope and channel sediment dynamics in the Clearwater River, western Washington State: Earth and Planetary Science Letters, v. 264, p. 123–135, doi: 10.1016/j.epsl.2007.09.013.

Bierman, P., and Steig, E., 1996, Estimating rates of denudation using cosmogenic isotope abundances in sediment: Earth Surface Processes and Landforms, v. 21, p. 125–139, doi: 10.1002/(SICI)1096-9837(199602)21:2<125::AID-ESP511>3.0.CO;2-8.

Binnie, S., Phillips, W., Summerfield, M., and Fairfield, L.K., 2007, Tectonic uplift, threshold hillslopes and denudation rates in a developing mountain range: Geology, v. 35, p. 743–746, doi: 10.1130/G23641A.1.

Braun, J., 2005, Quantitative constraints on the rate of landform evolution derived from low-temperature thermochronology: Reviews in Mineralogy and Geochemistry, v. 58, p. 351–374, doi: 10.2138/rmg.2005.58.13.

Brown, E.T., Stallard, R.F., Larsen, M.C., Bourles, D.L., Raisbeck, G.M., and Yiou, R., 1998, Determination of predevelopment denudation rates of an agricultural watershed (Cayaguas River, Puerto Rico) using in-situ–produced ^{10}Be in river-borne quartz: Earth and Planetary Science Letters, v. 160, p. 723–728, doi: 10.1016/S0012-821X(98)00123-X.

Bryant, B., 1990, Geologic map of the Salt Lake City 30′ × 60′ quadrangle, north-central Utah, and Uinta County, Wyoming: U.S. Geological Survey Miscellaneous Investigations Series Map I-1944, scale 1:100,000.

Burbank, D., Leland, J., Fielding, E., Anderson, R., Brozovic, N., Reid, M., and Duncan, C., 1996, Bedrock incision, rock uplift and threshold hillslopes in the northwestern Himalayas: Nature, v. 379, p. 505–510, doi: 10.1038/379505a0.

Chang, W.L., and Smith, R.B., 2002, Integrated seismic-hazard analysis of the Wasatch Front, Utah: Bulletin of the Seismological Society of America, v. 92, p. 1904–1922, doi: 10.1785/0120010181.

Cyr, A.J., and Granger, D.E., 2008, Dynamic equilibrium among erosion, river incision, and coastal uplift in the northern and central Apennines, Italy: Geology, v. 36, p. 103–106, doi: 10.1130/G24003A.1.

Davis, F.D., 1983, Geologic map of the central Wasatch front, Utah: Utah Geological Survey Map 54-A, scale 1:100,000.

Ehlers, T.A., 2005, Crustal thermal processes and thermochronometer interpretation: Reviews in Mineralogy and Geochemistry, v. 58, p. 315–350, doi: 10.2138/rmg.2005.58.12.

Ehlers, T.A., and Chan, M.A., 1999, Tidal cyclicities and estuarine deposition of the Proterozoic Big Cottonwood Formation, Utah: Journal of Sedimentary Research, v. 69, p. 1169–1180.

Ehlers, T.A., and Farley, K.A., 2003, Apatite (U-Th)/He thermochronometry: Methods and applications to problems in tectonic and surface processes: Earth and Planetary Science Letters, v. 206, p. 1–14, doi: 10.1016/S0012-821X(02)01069-5.

Ehlers, T.A., Willett, S.D., Armstrong, P.A., and Chapman, D.S., 2003, Exhumation of the central Wasatch Mountains, Utah: 2. Thermokinematic model of exhumation, erosion, and thermochronometer interpretation: Journal of Geophysical Research, v. 108, doi: 10.1029/2001JB001723.

Farley, K.A., 2000, Helium diffusion from apatite: General behavior as illustrated by Durango fluorapatite: Journal of Geophysical Research, v. 105, p. 2903–2914, doi: 10.1029/1999JB900348.

Frankel, K.L., and Pazzaglia, F.J., 2005, Tectonic geomorphology, drainage basin metrics, and active mountain fronts: Geografia Fisica e Dinamica Quaternaria, v. 28, p. 7–21.

Friedrich, A.M., Wernicke, B.P., Niemi, N.A., Bennett, R.A., and Davis, J.L., 2003, Comparison of geodetic and geologic data from the Wasatch region, Utah, and implications for the spectral character of Earth deformation at periods of 10 to 10 million years: Journal of Geophysical Research, v. 108, doi: 10.1029/2001JB000682.

Gosse, J.C., and Phillips, F.M., 2001, Terrestrial in situ cosmogenic nuclides: Theory and application: Quaternary Science Reviews, v. 20, p. 1475–1560, doi: 10.1016/S0277-3791(00)00171-2.

Granger, D.E., Kirchner, J.W., and Finkel, R.C., 1996, Spatially averaged long-term erosion rates measured from in situ-produced cosmogenic nuclides in alluvial sediment: The Journal of Geology, v. 104, p. 249–257.

Hales, T.C., and Roering, J.J., 2007, Climate controls on frost cracking and implications for the evolution of bedrock landscapes: Journal of Geophysical Research, v. 112, doi: 10.1029/2006JF000616.

Heisinger, B., Lal, D., Jull, A.J.T., Kubik, S., Ivy-Ochs, S., Neumaier, S., Knie, K., Lazarev, V., and Nolte, E., 2002a, Production of selected cosmogenic radionuclides by muons: 1. Fast muons: Earth and Planetary Science Letters, v. 200, p. 345–355, doi: 10.1016/S0012-821X(02)00640-4.

Heisinger, B., Lal, D., Jull, A.J.T., Kubik, S., Ivy-Ochs, S., Knie, K., and Nolte, E., 2002b, Production of selected cosmogenic radionuclides by muons: 2. Capture of negative muons: Earth and Planetary Science Letters, v. 200, p. 357–369, doi: 10.1016/S0012-821X(02)00641-6.

Howard, A.D., Dietrich, W.E., and Seidl, M.A., 1994, Modeling fluvial erosion on regional to continental scales: Journal of Geophysical Research, v. 99, p. 13,971–13,986, doi: 10.1029/94JB00744.

Kirchner, J.W., Finkel, R.C., Riebe, C.S., Granger, D.E., Clayton, J.L., King, J.G., and Megahan, W.F., 2001, Mountain erosion over 10 yr, 10 k.y., and 10 m.y. time scales: Geology, v. 29, p. 591–594, doi: 10.1130/0091-7613(2001)029<0591:MEOYKY>2.0.CO;2.

Kowallis, B.J., Ferguson, J., and Jorgensen, G.J., 1990, Uplift along the Salt Lake segment of the Wasatch fault from apatite and zircon fission track dating in the Little Cottonwood Stock: Nuclear Tracks and Radiation Measurements, v. 17, p. 325–329, doi: 10.1016/1359-0189(90)90054-2.

Laabs, B.J.C., Plummer, M., and Mickelson, D.M., 2006, Climate during the last glacial maximum in the Wasatch and southern Uinta Mountains inferred from glacier modeling: Geomorphology, v. 75, p. 300–317, doi: 10.1016/j.geomorph.2005.07.026.

Lund, W.R., 2005, Consensus Preferred Recurrence-Interval and Vertical Slip-Rate Estimates: Review of Utah Paleoseismic-Trenching Data by the Utah Quaternary Fault Parameters Working Group: Utah Geological Survey Bulletin 134, 109 p.

Machette, M.N., 1981, Preliminary investigations of late Quaternary slip rates along the southern part of the Wasatch fault zone, central Utah, *in* Hays, W.W., and Gori, P.L., eds., Proceedings of Conference XXVI; A Workshop on Evaluation of Regional and Urban Earthquake Hazards and Risk in Utah: U.S. Geological Survey Professional Paper 1275, p. 391–406.

Machette, M.N., Personius, S.F., and Nelson, A.R., 1992, Paleoseismology of the Wasatch fault zone: A summary of recent investigations, interpretations, and conclusions, *in* Gori, P.L., and Hays, W.W., eds., Assessment of Regional Earthquake Hazards and Risk Along the Wasatch Front, Utah: U.S. Geological Survey Professional Paper 1500, p. A1–A71.

Madsen, D.B., and Currey, D.R., 1979, Late Quaternary glacial and vegetation changes, Little Cottonwood Canyon area, Wasatch Mountains, Utah: Quaternary Research, v. 12, p. 254–270, doi: 10.1016/0033-5894(79)90061-9.

Matmon, A., Bierman, P.R., Larsen, J., Southworth, S., Pavich, M., and Caffee, M., 2003, Temporally and spatially uniform rates of erosion in the southern Appalachian and Great Smoky Mountains: Geology, v. 31, p. 155–158, doi: 10.1130/0091-7613(2003)031<0155:TASURO>2.0.CO;2.

Mattson, A., and Bruhn, R.L., 2001, Fault slip rates and initiation age based on diffusion equation modeling: Wasatch fault zone and eastern Great Basin: Journal of Geophysical Research, v. 106, no. B7, p. 13,739–13,750, doi: 10.1029/2001JB900003.

McCalpin, J.P., and Nishenko, S.P., 1996, Holocene paleoseismicity, temporal clustering, and probabilities of future large (M > 7) earthquakes on the Wasatch fault zone, Utah: Journal of Geophysical Research, v. 101, p. 6233–6253, doi: 10.1029/95JB02851.

Montgomery, D.R., and Brandon, M.T., 2002, Topographic controls on erosion rates in tectonically active mountain ranges: Earth and Planetary Science Letters, v. 201, p. 481–489, doi: 10.1016/S0012-821X(02)00725-2.

Naeser, C.W., Bryant, B., Crittenden, M.D.J., and Sorensen, M.L., 1983, Fission-track ages of apatite in the Wasatch Mountains, Utah: An uplift study, *in* Miller, D.M., Todd, V.R., and Howard, K.A., eds., Tectonics and Stratigraphy of the Eastern Great Basin: Geological Society of America Memoir 157, p. 29–36.

Nelson, A.R., and Personius, S.F., 1993, Surficial geologic map of the Weber segment, Wasatch fault zone, Weber and Davis Counties, Utah: U.S. Geological Survey Miscellaneous Investigations Series Map I-2199, scale 1:50,000.

Niemi, N.A., Wernicke, B.P., Friedrich, A.M., Simons, M., Bennett, R.A., and Davis, J.L., 2004, BARGEN continuous GPS data across the eastern Basin and Range Province, and implications for fault system dynamics: Geophysical Journal International, v. 159, p. 842–862, doi: 10.1111/j.1365-246X.2004.02454.x.

Niemi, N.A., Oskin, M., Burbank, D.W., Heimsath, A.M., and Gabet, E.J., 2005, Effects of bedrock landslides on cosmogenically determined erosion rates: Earth and Planetary Science Letters, v. 237, p. 480–498, doi: 10.1016/j.epsl.2005.07.009.

Nishiizumi, K., Imamura, M., Caffee, M.W., Southon, J.R., Finkel, R.C., and McAninch, J., 2007, Absolute calibration of ^{10}Be AMS standards: Nuclear Instruments & Methods in Physics Research–Beam Interactions with Materials and Atoms, v. 258B, p. 403–413, doi: 10.1016/j.nimb.2007.01.297.

Parry, W.T., and Bruhn, R.L., 1987, Fluid inclusion evidence for minimum 11 km vertical offset on the Wasatch fault, Utah: Geology, v. 15, p. 67–70, doi: 10.1130/0091-7613(1987)15<67:FIEFMK>2.0.CO;2.

Reiners, P.W., and Brandon, M.T., 2006, Using thermochronology to understand orogenic erosion: Annual Review of Earth and Planetary Sciences, v. 34, p. 419–466, doi: 10.1146/annurev.earth.34.031405.125202.

Roering, J.J., Kirchner, J.W., Sklar, L.S., and Dietrich, W.E., 2001, Hillslope evolution by nonlinear creep and landsliding: An experimental study: Geology, v. 29, p. 143–146, doi: 10.1130/0091-7613(2001)029<0143:HEBNCA>2.0.CO;2.

Roering, J.J., Perron, J.T., and Kirchner, J.W., 2007, Hillslope morphology and functional relationships between topographic relief and denudation: Earth and Planetary Science Letters, v. 264, p. 245–258, doi: 10.1016/j.epsl.2007.09.035.

Schaller, M., and Ehlers, T.A., 2006, Limits to quantifying climate driven changes in denudation rates with cosmogenic radionuclides: Earth and Planetary Science Letters, v. 248, p. 153–167, doi: 10.1016/j.epsl.2006.05.027.

Schaller, M., von Blanckenburg, F., Hovius, N., and Kubik, P.W., 2001, Large-scale erosion rates from in situ–produced cosmogenic nuclides in European river sediments: Earth and Planetary Science Letters, v. 188, p. 441–458, doi: 10.1016/S0012-821X(01)00320-X.

Stock, G.M., Ehlers, T.A., and Farley, K.A., 2006, Where does sediment come from? Quantifying catchment erosion with detrital apatite (U-Th)/He thermochronometry: Geology, v. 34, p. 725–728, doi: 10.1130/G22592.1.

Stone, J.O., 2000, Air pressure and cosmogenic isotope production: Journal of Geophysical Research, v. 105, no. B10, p. 23,753–23,759, doi: 10.1029/2000JB900181.

Vance, D., Bickle, M., Ivy-Ochs, S., and Kubik, P.W., 2003, Erosion and exhumation in the Himalaya from cosmogenic isotope inventories of river sediments: Earth and Planetary Science Letters, v. 206, p. 273–288, doi: 10.1016/S0012-821X(02)01102-0.

von Blanckenburg, F., 2005, The control mechanisms of erosion and weathering at basin scale from cosmogenic nuclides in river sediment: Earth and Planetary Science Letters, v. 237, p. 462–479, doi: 10.1016/j.epsl.2005.06.030.

Whipple, K.X., 2001, Fluvial landscape response time: How plausible is steady-state denudation?: American Journal of Science, v. 301, p. 313–325, doi: 10.2475/ajs.301.4-5.313.

Willett, S.D., and Brandon, M.T., 2002, On steady states in mountain belts: Geology, v. 30, p. 175–178, doi: 10.1130/0091-7613(2002)030<0175:OSSIMB>2.0.CO;2.

Wittmann, H., von Blanckenburg, F., Kruesmann, T., Norton, K.P., and Kubik, P.W., 2007, Relation between rock uplift and denudation from cosmogenic nuclides in river sediment in the central Alps of Switzerland: Journal of Geophysical Research, v. 112, p. F04010, doi: 10.1029/2006JF000729.

Wobus, C., Heimsath, A., Whipple, K., and Hodges, K., 2005, Active out-of-sequence thrust faulting in the central Nepalese Himalaya: Nature, v. 434, p. 1008–1011, doi: 10.1038/nature03499.

MANUSCRIPT RECEIVED 4 AUGUST 2008
REVISED MANUSCRIPT RECEIVED 4 NOVEMBER 2008
MANUSCRIPT ACCEPTED 5 NOVEMBER 2008

Printed in the USA